Semicond. Sci. Technol. **22** (2007) 763–768 doi:10.1088/0268-1242/22/7/015

Simulation of the reverse *I–V* characteristics of the Schottky barrier radiation detector structures prepared on semi-insulating GaAs

P Boháček, F Dubecký and M Sekáčová

Institute of Electrical Engineering, Slovak Academy of Sciences, Dúbravská cesta 9, 84104 Bratislava, Slovakia

E-mail: pavol.bohacek@savba.sk

Received 30 March 2007, in final form 14 May 2007
Published 7 June 2007
Online at stacks.iop.org/SST/22/763

Abstract

The reverse current–voltage (*I–V*) characteristics of the Schottky barrier radiation detector structures prepared on semi-insulating gallium arsenide (SI GaAs) have been simulated using a modified thermionic field emission (TFE) model. In order to explain the charge–current transport, the effect of tunnelling and thermionic field emission together with the Schottky barrier lowering were considered taking into account the voltage drop on the quasi-neutral bulk region. The modified TFE model describes reverse *I–V* characteristics in the temperature range between 300 K and 360 K. An observed agreement between measured and simulated characteristics enabled us to determine the Schottky barrier height and specific resistance of the SI GaAs base from the theoretical simulation. The results of calculated resistivities are compared with resistivities determined by the van der Pauw method. The value of the Schottky barrier height is in good agreement with the previously published data. A much higher value of the calculated ohmic current compared to the current corresponding to the diode structure at a low bias/current region is revealed. A detected difference increases with increasing temperature. This fact led us to conclude that the current in the linear part of the *I–V* characteristics in the low bias region does not correspond to the ohmic transport, being linear; that is, in contradiction with the more generally considered view.

1. Introduction

Undoped semi-insulating (SI) gallium arsenide (GaAs) grown by the liquid encapsulated Czochralski (LEC) method appears to be one of the most promising materials for the fabrication of low-cost, fast and radiation-resistant detectors of charged particles and photons capable of operating at room temperature [1].

The radiation detector structure mostly consists of a blocking Schottky contact on the front surface and a blocking (Schottky) or ohmic metal contact on the opposite surface of the SI GaAs wafer. Parameters of the Schottky barrier SI GaAs radiation detector depend on the quality of the substrate material [2, 3] as well as the Schottky contact technology. Electrical transport in such structures is mostly explained by the thermionic emission charge transport process [3, 4]. Selected parameters of the Schottky barrier are obviously obtained from an initial part of the current–voltage (*I–V*) characteristic in the forward direction (e.g. [3]), noting limitations due to the series resistance effect [5]. Another way for an observation of the Schottky barrier height is to determine its value from the reverse *I–V* characteristics where the detector operates, as used, for example, in a stimulating study of Lee *et al* [6] for a similar structure based, however, on SI InP. Progressive development of the SI GaAs radiation detector relates to a new kind of ohmic contact, called

'non-alloyed', introduced by Alietti *et al* [7]. Developed technology resulted in substantial increasing of the breakdown voltage and lowering of the saturation current. Improved performance of radiation detectors with such an electrode was published by Nava *et al* [8], who demonstrated an operation of the SI GaAs detector in full depletion. However, physical mechanisms of these observations are still not completely understood and explained until the present day following, for example, the remarks published in [9] and [10]. In this respect a new more detailed study of the electrical charge transport in SI GaAs is necessary. The present work is our first approach in this task.

In a comparison of GaAs with Si radiation detectors, there are two key differences. Absorption efficiency is controlled by the atomic number of the base material. From this point of view, Si is preferably used for detection of low energy photons up to about 20 keV which presents the main limitation of Si. GaAs is useful for detection of hard x-rays currently up to 100–200 keV, depending on particular detector topology (top/side irradiation). Concerning electrical characteristics, the SI form of Si is not used or even does not exist. For radiation detectors, high purity Si material is used with low free carrier concentration, less than 10^{13} cm^{-3}. Such a kind of Si radiation detector is used for spectrometry and also for low energy photon applications (mammography, x-ray diffraction). Hence, the bulk SI GaAs seems to be a unique material for detectors in modern digital radiology applications with good absorption efficiency, possibility of full depletion with low leakage current at room temperature operation, fast reaction rate and well-developed technology.

In our present work, a simple model based on the thermionic field emission (TFE) theory, taking into account the Schottky barrier lowering and tunnelling effects on the reverse *I–V* characteristics of SI GaAs radiation detector structures with the double Schottky back-to-back barriers, is used. Basing on numerical simulation, the Schottky barrier height and resistivity of the base substrate material are calculated. The calculated resistivities are compared with the values obtained from the conductivity measurements performed on the SI GaAs substrates at different temperatures.

2. Theoretical model

Let us consider a model of undoped SI GaAs in which net shallow acceptors are overcompensated by deep native EL2 donors with an energy level $E_C - E_{EL2} = 0.75$ eV [3]. Due to the band bending [11] in the reverse-biased Au–SI GaAs interface, the EL2 states in a part of the depletion region close to the interface become fully positively ionized, forming a space-charge layer. In such a case, the reverse voltage on the structure terminals is divided into voltage drops across the reverse-biased barrier, quasi-neutral bulk and forward-biased barrier. The voltage drop across the forward-biased barrier is neglected because it is very small.

The reverse current I_r of the structure described can be evaluated by [6]

$$I_r = \frac{A^* A_e T (\pi q E_{00})^{1/2}}{k_B} [q(V_r - I_r R_b) - (E_C - E_F) + \Phi_{b0}]^{1/2} \times \exp\left(-\frac{\Phi_{b0}}{k_B T}\right), \quad (1)$$

where A^* is the effective Richardson constant, A_e is the area of the Schottky barrier structure, T is the absolute temperature, k_B is the Boltzmann constant, E_F is the Fermi level, E_C is the lower edge of the conduction band, Φ_{b0} is the Schottky energy barrier height, V_r is the reverse bias voltage on the structure terminals, R_b is the quasi-neutral bulk resistance and q is the electronic charge.

The tunnelling parameter E_{00} is defined by the formula [6]

$$E_{00} = \frac{h}{4\pi}\left(\frac{N_D}{m^* \varepsilon_0 \varepsilon_r}\right)^{1/2}, \quad (2)$$

where N_D is the concentration of the shallow donors, m^* is the effective mass of the electron, h is the Planck constant, ε_0 is the permittivity of vacuum and ε_r is the relative permittivity.

If the lowering of the barrier $\Delta\Phi$ due to the electric field (the Schottky effect) is considered, Φ_{b0} in equation (1) should be replaced by $\Phi_{b0} - \Delta\Phi$, where

$$\Delta\Phi = \left(\frac{qE}{4\pi\varepsilon_0\varepsilon_r}\right)^{1/2}, \quad (3)$$

with the electric field

$$E = \left(\frac{2qN_d V_r}{\varepsilon_0 \varepsilon_r}\right)^{1/2}. \quad (4)$$

In our simulation, we assume the Schottky barrier lowering $\Delta\Phi$ from equations (3) and (4).

The constant B_k can be defined as follows:

$$B_k = \frac{1}{\pi E_{00}}\left(\frac{k_B}{qA^* A_e T}\right)^2 \quad (5)$$

and after transformation, equation (1) can be rewritten as

$$V_r = B_k \exp\left[\frac{2q(\Phi_{b0} - \Delta\Phi)}{k_B}\right] I_r^2 + R_b I_r + E_C - E_F - \Phi_{b0} + \Delta\Phi. \quad (6)$$

The $E_C - E_F$ value in equation (6) can be approximated by $E_g/2$, where E_g is the energy band gap width. The temperature dependence of E_g is used as follows [12]:

$$E_g(T) = E_g(300) - 0.000\,43(T - 300)\ . \quad (7)$$

Formula (6) has two unknown parameters, Φ_{b0} and R_b. For an evaluation of these parameters, a least squares fitting method was used to find a minimum of the function f:

$$f = \sum_{i=1}^{N} (V_r - V_{ri})^2. \quad (8)$$

The partial derivations of the function f are zero at a local extremum

$$\frac{\partial f(R_b, \Phi_{b0}, V_{ri}, I_{ri})}{\partial R_b} = 0, \quad \frac{\partial f(R_b, \Phi_{b0}, V_{ri}, I_{ri})}{\partial \Phi_{b0}} = 0, \quad (9)$$

where I_{ri} and V_{ri} are measured current and voltage values, respectively.

The nonlinear system of equations (9) was solved by the Newton–Raphson method [13], based on the linearization of the equations. The unknown parameters of the system with a

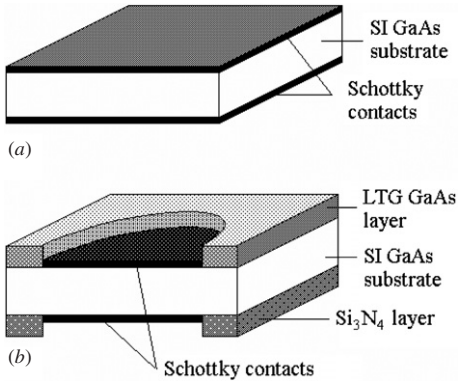

Figure 1. A perspective view of the back-to-back Schottky SI GaAs radiation detector structures: (*a*) without passivation layer and (*b*) with the LTG GaAs layer on the top and the Si_3N_4 layer on the back side respectively.

chosen tolerance are found by iteration:

$$\begin{pmatrix} R_{b,k+1} \\ \Phi_{b,k+1} \end{pmatrix} = \begin{pmatrix} R_{b,k} \\ \Phi_{b,k} \end{pmatrix} - \frac{1}{D} \begin{pmatrix} \dfrac{\partial^2 f}{\partial R_b^2} & -\dfrac{\partial^2 f}{\partial R_b \partial \Phi_{b0}} \\ -\dfrac{\partial^2 f}{\partial \Phi_{b0} \partial R_b} & \dfrac{\partial^2 f}{\partial \Phi_{b0}^2} \end{pmatrix}_k \times \begin{pmatrix} \dfrac{\partial f}{\partial R_b} \\ \dfrac{\partial f}{\partial \Phi_{b0}} \end{pmatrix}_k , \tag{10}$$

where

$$D = \left(\frac{\partial^2 f}{\partial R_b^2} \frac{\partial^2 f}{\partial \Phi_{b0}^2} - \frac{\partial^2 f}{\partial R_b \partial \Phi_{b0}} \frac{\partial^2 f}{\partial \Phi_{b0} \partial R_b} \right) . \tag{11}$$

The parameter values used in the simulation process were [7] $A^* = 4.4 \times 10^4$ A K^{-2} m^{-2}, $\varepsilon = 13.0$, $m^* = 0.068 m_0$ (m_0 is the mass of the free electron), $E_g(300) = 1.43$ eV and $N_D = 2.5 \times 10^{16}$ cm^{-3} from [3]. Other constants are well known.

3. Experimental details

The first group of samples consists of radiation detector structures without a passivation layer (figure 1(*a*)). Undoped LEC SI GaAs 2″ wafers with crystallographic orientation (1 0 0) and a thickness of 400 μm from two manufacturers—OMK (Slovakia) and Wacker Chemitronic (Germany)—were used for sample preparation. The wafer thickness of the first group of samples was reduced by lapping and chemo-mechanically polishing to 230 μm (OMK) and 250 μm (WA). The symmetrical back-to-back Schottky sandwich structures with semitransparent Au contacts were prepared by electron beam evaporation of Au in a high-vacuum deposition system (10^{-6} Pa). The samples were etched in HCl for 5 min, washed in deionized water and dried in nitrogen flow before evaporation. Samples with an area within the range 1.5–7 mm^2 were cleaved from the wafer and contacted by silver paste on a standard metallic transistor holder (TO 5).

The second group of samples represents detector structures with a passivation layer (figure 1(*b*)) with the aim to depress the surface leakage current. The wafers were used from four various manufacturers—American Xtal Technology (AXT), Outokumpu (OK), MCP Wafer Technology (MCP) and Showadenko (SD). The OK, MCP and SD wafers were prepared by LEC, while the AXT by the vertical gradient freeze (VGF) technology. The OK, MCP and AXT wafers were undoped and SD wafer was Cr doped. The molecular beam epitaxial layer grown at low temperature (250 °C) (LTG) on SI GaAs was used as a front-side passivation. The layer having a thickness of 500 nm was subsequently annealed *in situ* at 590 °C. A silicone nitride passivation layer with a thickness of 100 nm was prepared by sputtering of Si in N_2 atmosphere onto the back side. The circular windows with a diameter of 2 mm allowing contact deposition were formed in the LTG GaAs and silicone nitride passivation using etching in an O_2 plasma through the lift-off photoresist mask formed by double-sided photolithography. Metal Schottky contacts (Ti/Au) were evaporated by electron gun onto freshly etched wafers (HCl:H_2O = 1:2) after opening the windows. The Schottky contacts were formed on both sides through the photoresist mask using the lift-off technique.

The reverse *I–V* characteristics of the radiation detector structures were measured in a dark and electrically shielded probe station in a temperature range of 300–360 K (step of 20 K) using an HP 4140B pA metre/dc voltage source controlled by a personal computer through the GPIB bus. The base material resistivity was determined from conductivity measurements using the van der Pauw method in the same temperature steps. Before the measurement, the samples were chemically etched in a solution of $4H_2SO_4$:$1H_2O_2$:$1H_2O$ for 3 min, rinsed in deionized water and subsequently treated in HCl to avoid undesired oxides and again rinsed in deionized water. The electrical contacts in the corners of the square-shaped samples (10 mm × 10 mm) were prepared by the rubbing of a Ga+In eutectic alloy into the surface of the sample at room temperature, and their ohmic behaviour was confirmed by the measurement of *I–V* characteristics. Precise dc conductivity measurements were carried out using a digital electrometer Keithley 619. The maximal 5% error was estimated in the determination of the conductivity using the van der Pauw method.

4. Results and discussion

The values of measured and calculated current were recalculated to the current density J, using a known contact area for all investigated samples. The results of measurement and simulation are shown in figures 2(*a*) and (*b*) for OMK and in figures 3(*a*) and(*b*) for WA samples without the passivation layer, in both cases. The simulated curves are marked by the dotted lines and measured values by the solid ones. The current density–voltage (*J–V*) curves are plotted in log–lin scales (figures 2(*a*) and 3(*a*)), as a function of the temperature in a range of 300–360 K, with a step of 20 K. The *J–V* characteristics of the same samples are plotted in log-log scales in figures 2(*b*) and 3(*b*), respectively. The dashed straight lines correspond to linear-ohmic transport calculated from conductivity measurements. The display of *J–V* characteristics in the two plots is important, because the log–log plot shows in details the low bias voltage region while the high bias voltage region is better pronounced in the log–lin plot. For all the temperatures, the current densities in figure 2(*b*) show similar

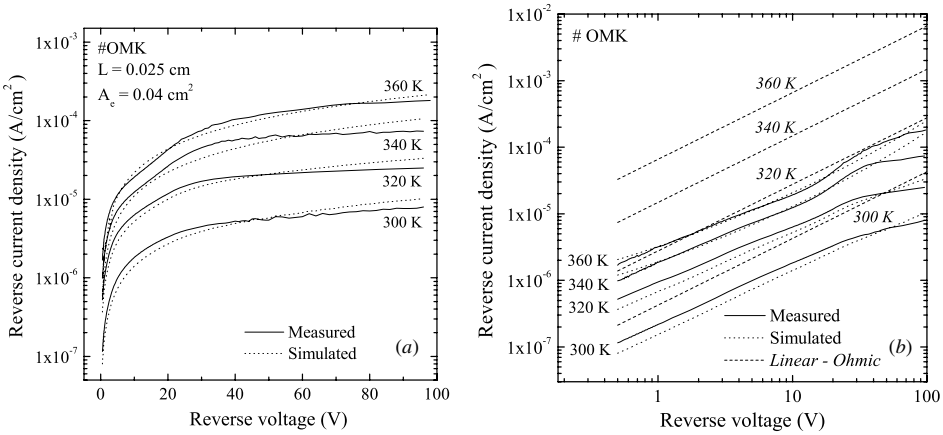

Figure 2. Measured (solid line) and simulated (broken line) reverse *J–V* characteristics of the radiation detector structure (OMK) without the passivation layer in the temperature range from 300 to 360 K (*a*) in the semi-log plot and (*b*) in the log–log plot. The dashed straight lines (*b*) correspond to the linear-ohmic transport calculated from the conductivity measurements.

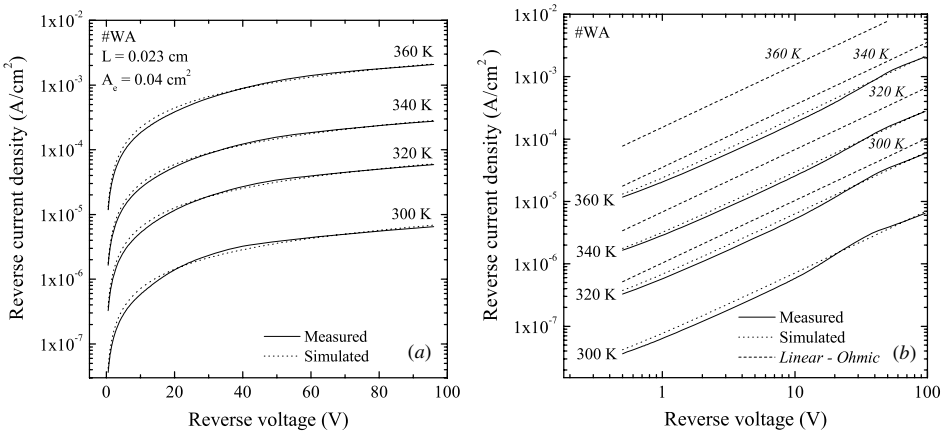

Figure 3. Measured (solid line) and simulated (broken line) reverse *J–V* characteristics of the radiation detector structure (Wacker) without the passivation layer in the temperature range from 300 to 360 K (*a*) in the semi-log plot and (*b*) in the log–log plot. The dashed straight lines (*b*) correspond to the linear-ohmic transport calculated from conductivity measurements.

Table 1. Calculated and measured results for variable temperatures and for samples OMK and Wacker without the passivation layer.

	OMK			Wacker		
T (K)	Φ_{b0} (eV)	ρ (measured) (Ω m)	ρ (simulated) (Ω m)	Φ_{b0} (eV)	ρ (measured) (Ω m)	ρ (simulated) (Ω m)
300	0.818	9.70×10^5	1.26×10^6	0.894	4.20×10^5	6.08×10^5
320	0.827	1.45×10^5	1.74×10^5	0.890	6.42×10^4	6.86×10^4
340	0.838	2.70×10^4	3.61×10^4	0.890	1.22×10^4	1.47×10^4
360	0.871	6.07×10^3	8.02×10^3	0.883	2.81×10^3	2.96×10^3

features which can be described as a function of the voltage in the following way: at low voltages, the curves show a slightly sublinear shape while at higher voltages over 70 V, a saturation of current densities is observed. The *J–V* dependences in figure 3(*b*) have almost a linear behaviour with a tendency to sublinear (saturation) at about 40 V. It can be seen from figures 2 and 3 that the experimental results are in good agreement with the simulated values for both samples.

An uncertain parameter in the simulation relates to the concentration of EL2 traps N_T that overcompensate the shallow acceptors N_A. We evaluated the influence of this parameter on the simulation of *J–V* characteristics and calculated values of the barrier height and resistivity. The change of N_D within the range $\langle 1 \times 10^{16}$ cm^{-3}, 5×10^{16} cm$^{-3}\rangle$ caused negligible changes in the simulated *J–V* characteristics. The difference lies below 5% and 0.5% for the barrier height and the resistivity, respectively. The values of the measured resistivities and the resistivities and barrier heights calculated from our modified TFE model are presented in table 1 for both samples. The values obtained for the Schottky barrier height for the samples without the passivation layer are $\Phi_{b0} = (0.83 \pm 0.02)$ eV (OMK) and $\Phi_{b0} = (0.89 \pm 0.01)$ eV (WA). The obtained value of sample WA is in excellent agreement with the published data for Au on N-type (1 0 0) GaAs (e.g. 0.87 eV and 0.89 eV [11]). The calculated resistivity of sample OMK is about 30% greater than the

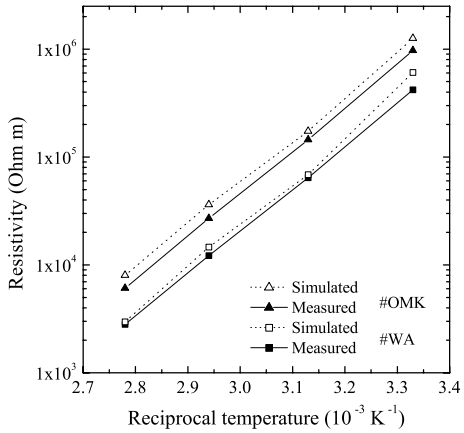

Figure 4. The dependence of electrical resistivity versus reciprocal temperature obtained from conductivity measurements (solid triangle and square) and from simulation (open triangle and square) for OMK and Wacker samples, respectively.

measured resistivity. The calculated resistivity of sample WA is greater than the measured resistivity (7–45%), depending on particular temperatures. Considering the simplicity of the model, such deviations seem to be acceptable.

The logarithm of the measured resistivity ρ as a function of the reciprocal absolute temperature, shown in figure 4 (solid triangles and squares), gave parallel straight lines (the slope is practically the same) indicating the existence of the traps lying below the lower edge of the conduction band. The activation energy E_a of the traps is nearly the same; 0.687 eV and 0.678 eV were obtained from the Arrhenius plot log (ρ) versus $1/T$. The simulated values of the resistivity are plotted by open symbols.

The reverse *J–V* characteristics of the detector structures with the passivation layer are shown in figures 5(*a*) and (*b*) for various samples plotted in the semilog and log–log scales, respectively. The measured (solid line) and calculated (broken line) curves were obtained at 300 K. The dashed straight lines correspond to the linear-ohmic transport calculated from conductivity measurements in figure 5(*b*). The

Table 2. Calculated and measured results for samples of various producers with the passivation layer and for a temperature of 300 K.

Samples of SI GaAs	Φ_{b0} (eV)	ρ (measured) (Ω m)	ρ (simulated) (Ω m)
AXT	0.793	2.64×10^5	5.13×10^5
OK	0.795	1.45×10^5	3.05×10^5
MCP	0.801	8.81×10^5	1.18×10^6
SD	0.815	1.20×10^6	3.53×10^6

J–V curves are almost linear at low voltages, with a slight tendency towards a sublinear shape. Deviation towards the sublinear shape starts for all samples at a bias voltage higher than 9–12 V. The lowest reverse current density shows the Cr-doped sample SD that is comparable with the samples without the passivation layer. The highest current densities are observed in the samples AXT and OK. The values of the measured and calculated resistivities and calculated barrier heights are listed in table 2. The barrier height obtained for passivated samples gives the value $\Phi_{b0} = (0.80 \pm 0.01)$ eV that is slightly lower than the published data for Au on N-type GaAs [11]. The barrier height change confirms a non-negligible contribution of the leakage surface current to the total current of the SI GaAs structure with a blocking barrier. On the other hand, additional current influences the calculated value of the barrier height. Due to this contribution, calculated values of the unpassivated Schottky barrier structures give an apparent, lower value of the barrier height. The electrode geometry of the radiation detector is of the order of 100 μm; hence the metal–semiconductor interface micro-inhomogeneities [14] create an integral contribution to the leakage current. The calculated barrier height determined from the experimental *I–V* characteristic is influenced by this contribution; therefore an apparent effective barrier height value is observed. The calculated resistivities are greater than the measured resistivities (0.3–2 times) for particular samples. This discrepancy between the calculated and measured resistivities may be partially caused by using different samples in conductivity measurements and simulations. Additionally, more parameters play a role in the determination of the

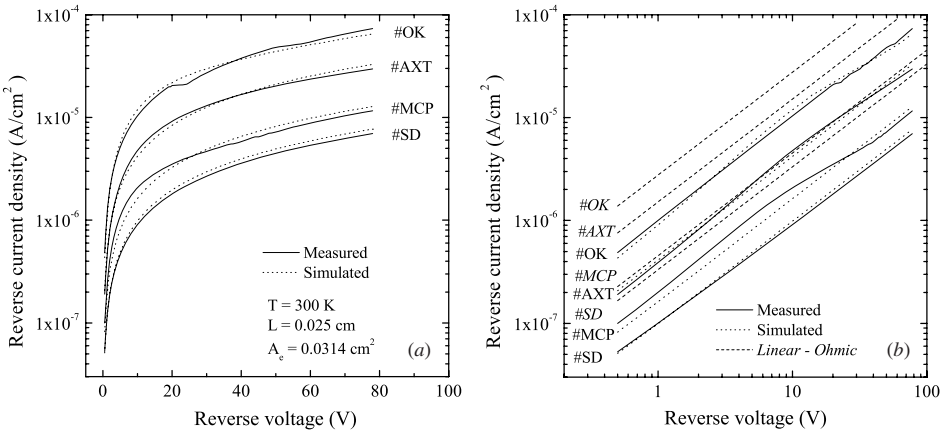

Figure 5. Measured (solid lines) and simulated (broken lines) reverse *J–V* characteristics of radiation detector structures with the passivation layer on SI GaAs from four various manufacturers at 300 K (*a*) in the semi-log plot and (*b*) in the log–log plot. The dashed straight lines (*b*) correspond to the linear-ohmic transport calculated from conductivity measurements.

resistivity from simulations that can affect the accuracy of the calculation. Such parameters include inhomogeneities and defects presented on the metal–semiconductor interface, surface leakage currents, instability and lower accuracy of the measurement of temperature in *I–V* measurements, approximated location of E_F, concentration of deep states of EL2 and choice of the set of experimental points for simulation. As is seen from the results of the simulation, the used TFE model is better applicable for samples having passivation because of their well-defined dimensions. In addition, the edge leakage current of these samples is suppressed by LTG GaAs and Si_3N_4 passivation layers.

5. Conclusion

Modified thermionic field emission theory has been formulated and used on SI GaAs Schottky barrier structures in a way that is new and easy to simulate and to compare with experimental data. The TFE model with the Schottky barrier lowering effect and tunnelling in SI GaAs Schottky barrier detector structures has been shown to be suitable for both types of the samples without and with the passivation layer in the temperature range from 300 to 360 K. Reverse current density–voltage characteristics, Schottky barrier height and electrical resistivity have been calculated using the proposed theoretical model and compared with the measured data. The experimental results are in good agreement with the simulated values for all investigated samples. From these results, we can conclude that in the back-to-back Schottky barrier structures studied based on SI GaAs the dominating charge-carrier transport corresponds to the applied modified TFE model. However, following a preliminary observation, the TFE model in the present form cannot be applied in the SI GaAs structure with a new ohmic contact (using defective interface) as used by Alietti *et al* [7].

Acknowledgments

The authors acknowledge M Krempaský and R Senderák for assistance in technology and I Bešše for stimulation and helpful discussion. This work was supported in a part through grants of the Scientific Grant Agency (VEGA) No. 2/7170/27 and Agency for Support of Science and Research No. APVT-99-P06305.

References

[1] Schlesinger T E and James R B 1995 *Semiconductors for room temperature nuclear detector applications Semiconductors and Semimetals* vol 43 ed R K Wilardson, A C Beer and E R Weber (San Diego: Academic)
[2] Dubecký F, Ferrari C, Korytár D, Gombia E and Nečas V 2007 *Nucl. Instrum. Methods* A **576** 27–31
[3] Baldini R, Vanni P, Nava F, Canali C and Lanzieri C 2000 *Nucl. Instrum. Methods* A **449** 268–76
[4] Cola A 1996 *Proc. 3rd Int. Workshop on GaAs and Related Compounds* ed P G Pelfer, J Ludwig, K Runge and H S Rupprecht (Singapore: World Scientific) p 217
[5] Aubry V and Meyer F 1994 *J. Appl. Phys.* **76** 7973–84
[6] Lee T C, Au H L, Chen T P, Ling C C, Fung S and Beling C D 1993 *Semicond. Sci. Technol.* **8** 709–11
[7] Alietti M *et al* 1995 *Nucl. Instrum. Methods* A **362** 344–8
[8] Nava F, Bertuccio G, Vanni P, Canali C, Cavallini A, Castaldini A and Polenta L 1997 *IEEE Trans. Nucl. Sci.* **44** 943–9
[9] Cola A, Reggiani L and Vasanelli L 1997 *Semicond Sci. Technol.* **12** 1358–64
[10] Castaldini A, Cavallini A, Polenta L, Canali C and Nava F 1998 *Nucl. Instrum. Methods* A **410** 79–84
[11] Rhoderick E H and Williams R H 1988 *Metal–Semiconductor Contacts* (Oxford: Clarendon)
[12] 1990 *Properties of Gallium Arsenide, EMIS Datareviews 2* (Surrey: Unwin Brothers)
[13] Demidovich B P and Maron I A 1987 *Computational Mathematics* (Moscow: Mir)
[14] Werner J H and Güttler H H 1991 *J. Appl. Phys.* **69** 1522–33